Ecological Informatics 56 (2020) 101040

Contents lists available at ScienceDirect

Ecological Informatics

journal homepage: www.elsevier.com/locate/ecolinf

A simpler way to predict flowering and full bloom dates of cherry blossoms by self-organizing maps

Shin Nagai[a,*], Hiroshi Morimoto[b], Taku M. Saitoh[c]

[a] Earth Surface System Research Center, Research Institute for Global Change, Japan Agency for Marine-Earth Science and Technology (JAMSTEC), 3173-25 Showa-machi, Kanazawa-ku, Yokohama 236-0001, Japan
[b] Nagoya University, Furo-cho, Chikusa-ku, Nagoya 464-8601, Japan
[c] River Basin Research Center, Gifu University, 1-1 Yanagido, Gifu 501-1193, Japan

ARTICLE INFO

Keywords:
Blooming phenology
Cherry
Climate change
Japan
Phenology model
Self-organizing maps

ABSTRACT

Knowledge of flowering and leaf flush phenology is important for a deep understanding of the responses of ecosystem functions, ecosystem services, and biodiversity to climate change. Process-based phenology models, which account statistically for chilling accumulation for endodormancy release and thermal accumulation after endodormancy release, can predict flowering and leaf flush dates, but they are difficult to develop for poorly studied species. A simpler approach is needed. We propose a model of the blooming phenology of Yoshino cherry trees (*Cerasus* ×*yedoensis*) based on bidirectional self-organizing maps (SOM). SOM, a data mining approach, is a tool for categorizing patterns in *n*-dimensional observation data by forming a two-dimensional lattice. The bidirectional SOM was applied to the data of daily mean temperature, using flowering (or full blooming) dates as teacher signals. We inputted daily mean air temperatures during the thermal accumulation period (mainly from February to just before flowering) into multiple input vectors and obtained flowering or full bloom dates into an output vector. The mean absolute errors between predicted and observed dates at 42 locations in Japan ranged from 2.8 to about 4.5 days for flowering and full bloom. The bidirectional SOM approach had a slightly higher error than the process-based phenology model approach, but it has an advantage in predicting flowering and leaf flush dates of poorly studied species under future warming conditions.

1. Introduction

Evaluation of the spatiotemporal variability of flowering and leaf flush dates is important for a deep understanding of the likely responses of ecosystem functions, ecosystem services, and biodiversity to climate change. Changes in flowering and leaf flush dates affect photosynthesis capacity and gross primary productivity (i.e., ecosystem functions; Peñuelas et al., 2009; Richardson et al., 2013), the scheduling of festivals and tourism (i.e., cultural ecosystem services; Sakurai et al., 2011; Sparks, 2014; Kim et al., 2015; Wang et al., 2017), and phenology alignment (e.g., flowering and pollinator activities; Kudo, 2014; Donnelly and Yu, 2017). In the mid to high latitudes of the Northern Hemisphere, long-term in situ observed data show the advance of flowering and leaf flush dates due to global warming (Badeck et al., 2004; Linderholm, 2006; Menzel et al., 2006). On the other hand, phenology models suggest that both may be delayed in some areas owing to insufficient chilling under future warming conditions (Harrington and Gould, 2015; Maruoka and Itoh, 2009). In either case, the sensitivity of flowering and leaf flush phenology to climate change differs along a latitudinal gradient (Wang et al., 2015a, 2015b).

To accurately evaluate the spatiotemporal variability of flowering and leaf flush dates under future climate change, we need suitable phenology models for each species in each area, based on long-term in situ observed data. The main factors underlying flowering and leaf flush are chilling accumulation for endodormancy release and thermal accumulation after endodormancy release (Basler, 2016; Cesaraccio et al., 2004; Chuine et al., 2016; Chung et al., 2011; Fu et al., 2012; Körner and Basler, 2010). Both differ among species (Basler, 2016; Cesaraccio et al., 2004; Fu et al., 2012).

Published process-based phenology models statistically evaluate various parameters that account for endodormancy and thermal accumulation processes (Chung et al., 2011; Fu et al., 2012; Luedeling et al., 2013). For instance, parameters that account for both processes of Yoshino cherry trees (*Cerasus* ×*yedoensis*) were evaluated in Japan

* Corresponding author at: Earth Surface System Research Center, Research Institute for Global Change, Japan Agency for Marine-Earth Science and Technology, 3173-25 Showa-machi, Kanazawa-ku, Yokohama, Kanagawa 236-0001, Japan.
E-mail addresses: nagais@jamstec.go.jp (S. Nagai), h.morimoto@nagoya-u.jp (H. Morimoto), taku@green.gifu-u.ac.jp (T.M. Saitoh).

https://doi.org/10.1016/j.ecoinf.2019.101040
Received 13 April 2019; Received in revised form 5 October 2019; Accepted 16 December 2019
Available online 18 December 2019
1574-9541/

Table 1
Summary of the start (D_{start}) and end dates (D_{end}) of bidirectional SOM analysis in Cases 1 and 2, and differences between each of flowering date and full bloom date and D_{end}. Means are shown in parentheses.

Area name	City	D_{start} in Case 2 (DOY)	D_{end} in Cases 1 & 2 (DOY)	Flowering date – D_{end} in Cases 1 & 2 (day)	Full bloom date – D_{end} in Cases 1 & 2 (day)
Hokkaido	Muroran	32	120	−7 – +26 (7.2)	−2 – +31 (12.0)
	Hakodate	1	110	−2 – +34 (12.1)	+1 – +38 (16.4)
Tohoku	Morioka	32	100	−1 – +27 (11.7)	+6 – +30 (16.4)
	Akita	32	100	−3 – +21 (9.3)	+2 – +28 (14.2)
	Sendai	1	90	−1 – +30 (11.3)	+4 – +35 (16.5)
	Yamagata	1	100	−7 – +20 (5.9)	−4 – +25 (10.6)
	Fukushima	1	90	−1 – +27 (9.5)	+3 – +30 (13.6)
Kanto	Mito	11	79	0 – +32 (14.1)	+8 – +39 (20.4)
	Utsunomiya	1	79	−2 – +30 (13.8)	+5 – +36 (19.9)
	Maebashi	32	79	0 – +27 (11.6)	+8 – +33 (18.7)
	Kumagaya	345[a]	79	−3 – +26 (10.4)	+2 – +32 (17.7)
	Chyoshi	32	79	−1 – +28 (10.9)	+8 – +35 (18.7)
	Tokyo	32	79	−4 – +23 (7.1)	+1 – +29 (15.1)
	Yokohama	32	79	−5 – +22 (7.2)	+2 – +27 (15.2)
Koshinetsu	Niigata	345[a]	90	0 – +28 (10.7)	+5 – +31 (15.8)
	Kofu	345[a]	79	−3 – +24 (9.0)	+2 – +28 (15.0)
	Nagano	1	100	−8 – +17 (3.1)	−5 – +23 (8.3)
Hokuriku	Toyama	1	90	−4 – +22 (6.9)	0 – +26 (11.4)
	Kanazawa	1	90	−4 – +19 (4.8)	+2 – +22 (10.1)
	Fukui	1	90	−4 – +19 (4.6)	+1 – +23 (9.4)
Tokai	Shizuoka	32	79	−5 – +18 (6.4)	+2 – +24 (14.6)
	Nagoya	32	79	−3 – +23 (7.7)	+7 – +27 (15.8)
	Gifu	32	79	−4 – +24 (8.5)	+6 – +28 (16.2)
Kinki	Hikone	1	90	−7 – +17 (3.4)	+2 – +25 (10.1)
	Kyoto	32	79	−2 – +21 (10.1)	+8 – +28 (17.4)
	Osaka	32	79	0 – +22 (9.6)	–
	Kobe	32	79	0 – +22 (9.9)	+8 – +26 (17.1)
	Wakayama	32	79	−4 – +18 (6.7)	–
Chugoku	Tottori	32	79	0 – +25 (12.3)	+8 – +29 (18.3)
	Okayama	345[a]	79	0 – +22 (10.5)	+8 – +27 (17.6)
	Matsue	32	90	−8 – +15 (1.7)	–
	Hiroshima	32	79	0 – +20 (8.5)	+7 – +28 (16.8)
	Shimonoseki	32	79	−2 – +18 (8.7)	+8 – +25 (17.2)
Shikoku	Takamatsu	1	79	−2 – +20 (9.7)	+3 – +27 (17.2)
	Matsuyama	32	79	−6 – +17 (7.2)	+6 – +26 (15.8)
	Tokushima	42	79	−2 – +18 (8.8)	+7 – +25 (16.5)
Kyushu	Fukuoka	32	79	−7 – +17 (5.6)	–
	Saga	32	79	−3 – +14 (5.6)	–
	Nagasaki	42	79	−5 – +13 (4.9)	+3 – +21 (14.0)
	Oita	32	79	−6 – +17 (6.8)	+5 – +24 (15.7)
	Kumamoto	32	79	−5 – +13 (4.3)	+2 – +21 (13.1)
	Kagoshima	60	79	−5 – +16 (6.6)	+6 – +26 (14.8)

[a] Previous year.

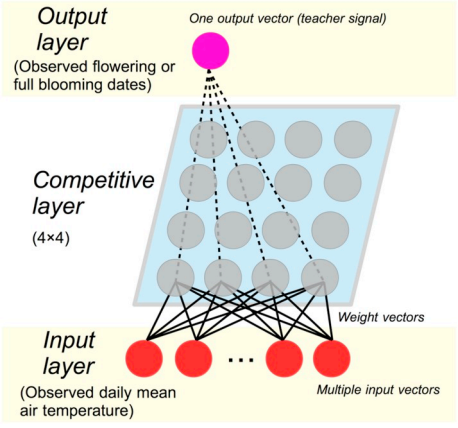

Fig. 1. Structure of the bidirectional SOM. We entered daily mean temperatures of 36 randomly selected years into multiple input vectors and observed flowering or full bloom dates into an output vector (teacher signal).

(Aono and Moriya, 2003; Asakura et al., 2010). However, the flowering and full bloom dates evaluated by these models showed high root mean square errors (RMSEs) at some sites with high mean air temperatures (Aono and Moriya, 2003; Asakura et al., 2010). In those models, parameters that account for dormancy processes used statistically best-fitted values collected during each study period. To achieve the long-term accuracy of process-based phenology models, parameter values must be based on long-term observed data.

Long-term phenological data observed at multiple sites are now published on websites (Templ et al., 2018; Wenden et al., 2016). Through their analysis, we can develop process-based phenology models that can predict the flowering and leaf flush dates for various species at multiple sites. However, the understanding of endodormancy and thermal accumulation processes for many species is still not enough (Basler, 2016; Chuine et al., 2016), so it is difficult to apply the approach to various species at multiple sites.

To solve these issues, we need a simple approach that does not require detailed knowledge of dormancy processes. Self-organizing maps (SOM), a tool for categorizing patterns in *n*-dimensional observation

data by forming a two-dimensional (2D) lattice (Kohonen, 1982, 1990), would allow us to predict the year-to-year variability of flowering and leaf flush dates by categorizing the pattern of daily mean temperature during endodormancy and thermal accumulation periods. We propose a new simple approach to predicting the flowering and full bloom dates of Yoshino cherry trees at multiple locations in Japan based on bidirectional SOM analysis of daily mean temperature and long-term in situ observed dates of flowering and full bloom.

2. Methods

2.1. Blooming phenology data

We used the dates of flowering (≥4 flowers open in an index tree) and full bloom (≳80% of flowers open in an index tree) from 1953 to 2018, which are published on the website of the Japan Meteorological Agency (JMA) (Japan Meteorological Agency (JMA), 2019a; Japan Meteorological Agency (JMA), 2019b). We targeted 42 locations for flowering date and 37 locations for full bloom date with complete data (Table 1).

2.2. Meteorological data

We used the daily mean and 10-day mean temperature data observed at 42 stations, where correspond closely to the flowering sites, of the JMA's Automated Meteorological Data Acquisition System (AMeDAS) (Japan Meteorological Agency (JMA), 2019c).

2.3. Self-organizing maps (SOM)

SOM analysis was introduced as a kind of cluster mapping (Kohonen, 1982, 1990). It aims to supply overviews of given multivariate data sets (input layer) by visualizing cluster tendency of the data over graphical map displays (competitive layer). It has been applied broadly in many fields, and has become a well researched technique of data mining (Gao et al., 2019; Hudson et al., 2011; Pérez-Hoyos et al., 2014).

Using artificial neural networks, SOM aims to provide continuous mapping from the input layer to a competitive layer (usually a 2D space). The competitive layer consists of a defined number of "neurons" and forms a 2D lattice that is easily visualized. These points in lattice in plane are also called "units". The map conserves the original structure of the measurement vectors in the *n*-dimensional space in the plane. As

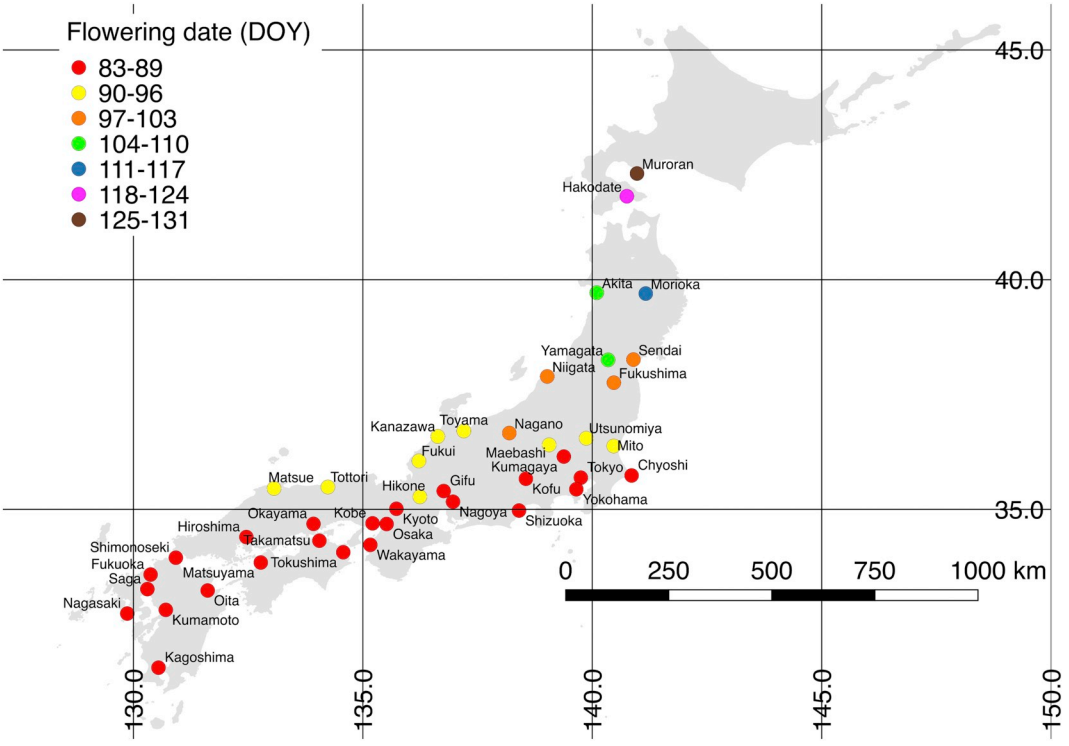

Fig. 2. Average (a) flowering and (b) full bloom dates of Yoshino cherry trees between 1953 and 2018.

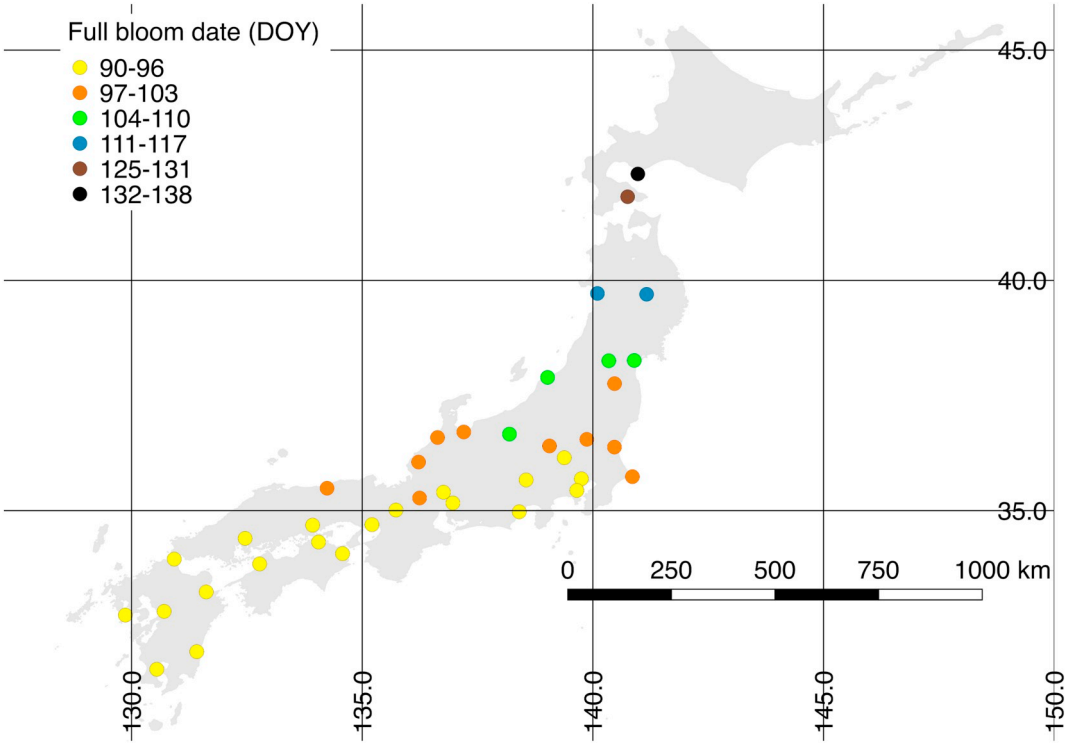

Fig. 2. (*continued*)

a result, if points in the original data are "near" (or "far"), then they are mapped to "near" (or "far") units in the plane. Thus SOM visualizes the tendency of clusters of the given data (Fig. 1). The basic principle behind the SOM algorithm is that the weight vectors of neurons, which are initialized randomly, come to represent a number of original measurement vectors during an iterative data input process.

SOM as used here is "bidirectional", being based on supervised neural learning algorithms with instruction signals as an output vector of the output layer.

2.4. Prediction of flowering dates

In the bidirectional SOM analysis, we input daily mean temperature into multiple input vectors and obtained flowering or full bloom dates into an output vector (teacher signal). We analyzed two cases of the input vector periods: Case 1, endodormancy and thermal accumulation periods, and Case 2, periods with a correlation between flowering date and temperature. As the flowering date of Yoshino cherry trees is correlated with the variability of temperature just before bloom (Kai et al., 1993; Miller-Rushing et al., 2007), we assumed that Case 2 might reduce the prediction accuracy more than Case 1 might.

Case 1. Endodormancy and thermal accumulation periods.

We set the start date of daily mean temperature input into input vectors (D_{start}) as 1 November in the preceding year. We set the end date (D_{end}) as between 20 and 31 March, reflecting 10-day time steps before flowering date. The differences between D_{end} and the earliest dates between 1953 and 2018 ranged from −8 to +34 days (flowering) and from −5 to +39 days (full bloom) (Table 1, a negative value means that the earliest date was later than D_{end}).

Case 2. Periods with a correlation between flowering date and temperature.

We calculated coefficients of correlations among flowering date and temperature in 10-day increments between 1 November in the preceding year and 10 April. D_{start} was set as the first date when the temperature during two consecutive 10-day time steps was correlated with the flowering date. D_{end} was set as in Case 1.

2.5. Bidirectional SOM analysis

We used a 4 × 4 lattice as a competitive layer in Cases 1 and 2. For the training data, we randomly selected 36 years between 1953 and 2018. For the testing data, we used the other 30 years. We performed the analysis 10 times and then calculated the mean absolute error (MAE) between predicted and observed flowering and full bloom dates for the training data. We used MAE because the effect of outliers on MAE is less than that on RMSE. In Shizuoka and Kobe, where complete data were not available for daily mean temperature, we targeted 64 years with complete data.

We conducted all analyses in R v. 3.13 software (R Project for Statistical Computing, 2019).

3. Results

3.1. Flowering and full bloom dates

The average flowering and full bloom dates of Yoshino cherry trees between 1953 and 2018 progressed northwards from late March to early May (Fig. 2). The differences between the earliest (in Kumamoto) and latest dates (in Muroran) were 43 and 39 days, respectively.

3.2. Relationship between bloom phenology and temperature

D_{start} in Case 2 is the first date when temperature during two consecutive 10-day periods was correlated with flowering date. At half of all locations it was day of year (DOY) 32 (1 Feb.) (Table 1). At most of the other locations it was DOY 1 (1 Jan.) or 11 (11 Jan.), at four locations it was DOY 345 in the preceding year, and at one it was DOY 60 (1 Mar.), and two locations it was DOY 42 (11 Feb.).

3.3. Prediction of flowering and full bloom dates

MAEs between predicted and observed dates in Case 1 ranged from 3.03 to 5.17 days (average: 3.71 days) for flowering and from 3.12 to 5.00 days (3.39 days) for full bloom (Fig. 3). Those in Case 2 ranged from 2.78 to 4.33 days (3.39 days) for flowering and from 2.77 to 4.76 days (3.49 days) for full bloom (Fig. 4). The differences between MAEs (Case 2 minus Case 1) ranged from −1.12 to +0.4 days

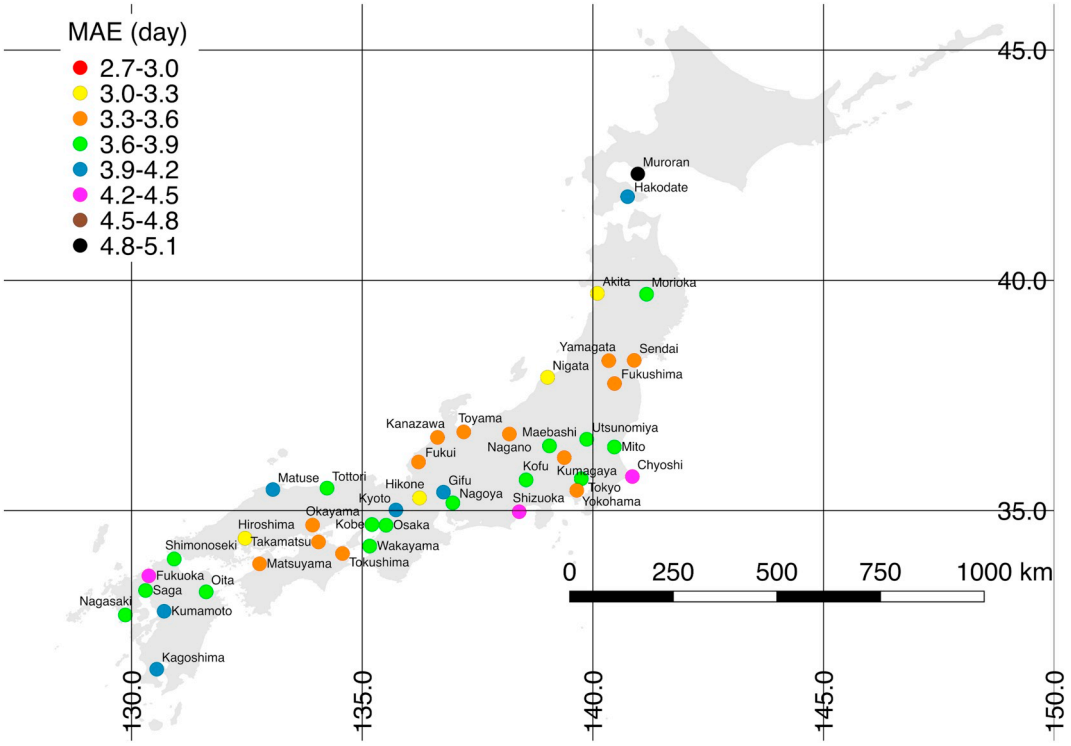

Fig. 3. Mean absolute errors (MAEs) between predicted and observed (a) flowering and (b) full bloom dates in Case 1 of bidirectional SOM analysis.

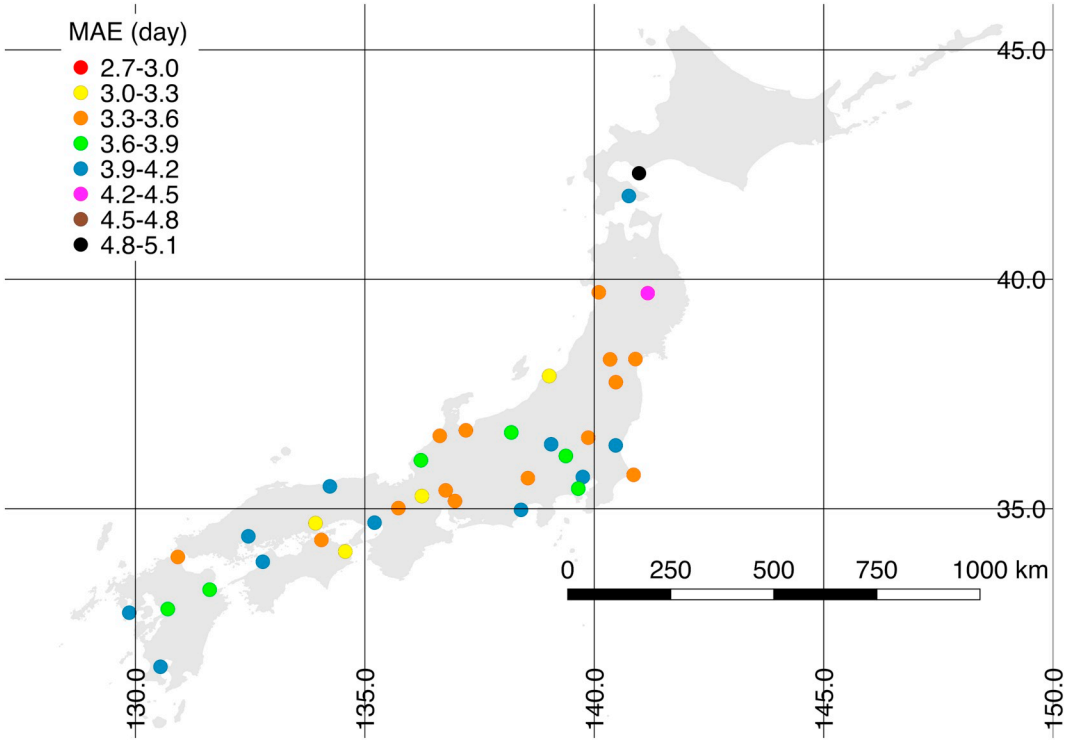

Fig. 3. (*continued*)

(−0.32 days) for flowering and from −0.7 to +0.7 days (−0.23 days) for full bloom. In most locations, MAE was smaller in Case 2 than in Case 1.

4. Discussion

In our proposed bidirectional SOM analysis, the MAE between predicted and observed flowering and full bloom dates was about 3 to 5 days (Fig. 3, 4). In previous process-based phenology models, the RMSEs were 2.8 days for flowering date (Aono and Moriya, 2003) and 1.65 to 4.11 days for full bloom date (Asakura et al., 2010). Thus, the bidirectional SOM analysis was slightly less accurate. However, it could predict dates of 1.7 to 14.1 days before the average flowering date and of 8.3 to 20.4 days before the full bloom date at each site (Table 1).

Being able to predict flowering and full bloom dates every year would support the planning of cultural events such as festivals and tourism. However, people need such dates more than a month ahead, for instance, the scheduling of extra trains to coincide with the flowering of red spider lily (*Lycoris radiata*) is planned 10 to 35 days ahead (Inoue and Nagai, 2015). To test the possibility of early prediction, we set D_{end} to 10 days before the values shown in Table 1 as an example. This reduced the prediction accuracy relative to Case 2 (periods with a correlation between flowering date and temperature as input): MAEs between predicted and observed flowering dates ranged from 3.26 to 5.21 days in Case 1 (daily mean temperature during endodormancy and thermal accumulation periods as input) and from 3.06 to 4.91 days in Case 2, and those between predicted and observed full bloom dates ranged from 3.34 to 5.25 days in Case 1 and from 2.86 to 5.20 days in Case 2. These results indicate that the prediction of these dates by bidirectional SOM analysis is difficult when 11.7 to 24.1 days before the average flowering date and 18.3 to 30.4 days before the average full bloom date. To predict flowering date earlier, we need another approach, such as Bayesian network analysis.

MAEs between predicted and observed flowering and full bloom dates by bidirectional SOM analysis were smaller in Case 2 (periods with a correlation between flowering date and temperature as input) than in Case 1 (daily mean temperature during endodormancy and thermal accumulation periods as input) (Fig. 3, 4). This result is supported by previous correlations of flowering and leaf flush dates with temperature during the thermal accumulation period (e.g., February or March, 1 to 2 months before flowering and leaf flush dates) (Fujisawa and Kobayashi, 2010; Jeong et al., 2011; Kai et al., 1993; Miller-

Rushing et al., 2007). The accuracy of prediction of the thermal accumulation period of six temperate tree species in central Europe under future warming by a process-based phenology model was equal to or better than that of the prediction of both endodormancy and thermal accumulation periods (Basler, 2016). These facts suggest that inputting daily mean temperature during the thermal accumulation period may improve the accuracy of prediction by bidirectional SOM analysis at sites where enough chilling is accumulated.

However, higher air temperatures in winter under future warming may further delay the date of endodormancy release, delaying flowering and full bloom. If the endodormancy period is positively correlated with flowering and full bloom dates, D_{start} should be set in November or December (i.e., during endodormancy period). In fact, we found a positive correlation between the average temperature from 11 to 20 November and flowering date in Kagoshima ($r = 0.38$, $P < .001$), with the highest annual mean air temperature of the study locations. MAEs between predicted and observed flowering and full bloom dates by bidirectional SOM analysis were smaller in Case 1 (daily mean temperature during endodormancy and thermal accumulation periods as input) than in Case 2 (periods with a correlation between flowering date and temperature as input) (Fig. 3, 4).

MAEs between predicted and observed flowering and full bloom dates were large at the locations where standard deviations (SD) of flowering and full bloom dates from 1953 to 2018 were large (Fig. 5). In contrast, SDs of monthly mean air temperature from 1953 to 2018 showed no geographical characteristic except for few locations in January and February (Fig. 6). These facts suggest a possibility that the locations with high year-to-year variability of flowering and full bloom dates may be affected by not only air temperature but also other factors. For instance, the model of flowering phenology in Aono and Moriya (2003) included the parameters that account for the horizontal distance between a target location and coastline and the ratio of sea area to a 31 km × 31 km grid mesh around the target location.

Process-based phenology models that do not account accurately for endodormancy had large prediction errors or underestimated leaf flush dates (Campoy et al., 2018; Luedeling et al., 2013). In contrast, the bidirectional SOM analysis allows us to incorporate endodormancy and thermal accumulation periods as one of patterns of SOM. Accordingly, we can succeed in avoiding uncertainties and errors caused by air temperature in winter season. In addition, its cost of calculation is low because we don't need to evaluate various parameters that for both processes. These advantages are useful for predicting the dates of flowering and leaf flush for poorly studied species under future warming.

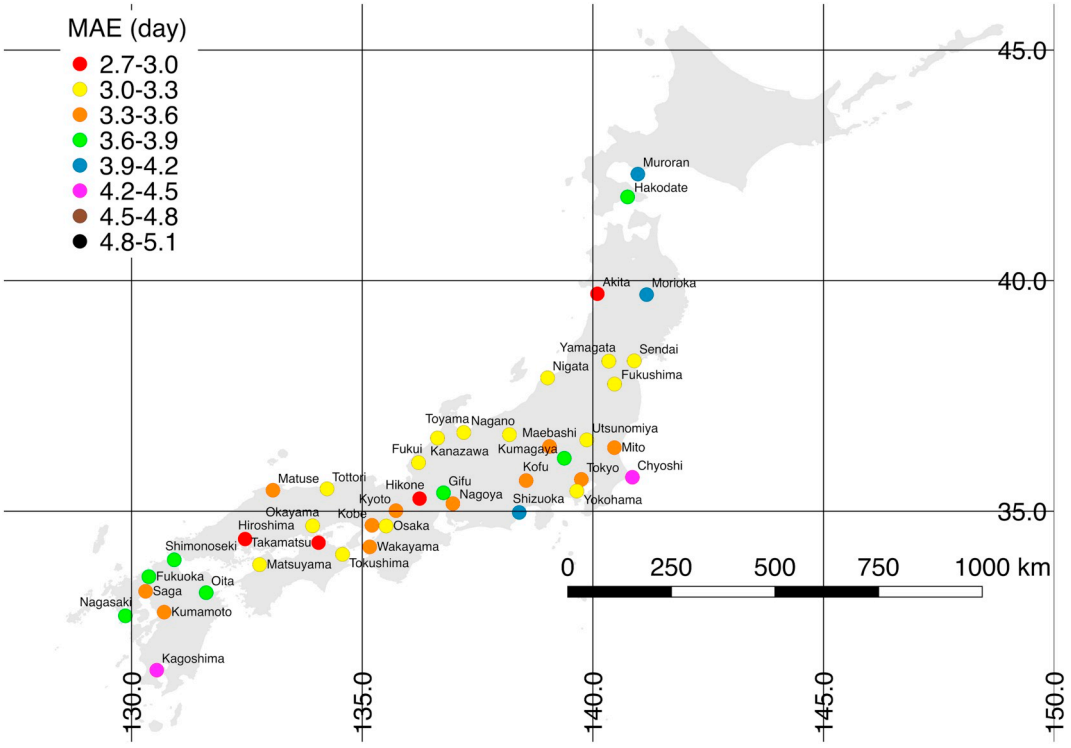

Fig. 4. MAEs between predicted and observed (a) flowering and (b) full bloom dates in Case 2 of bidirectional SOM analysis.

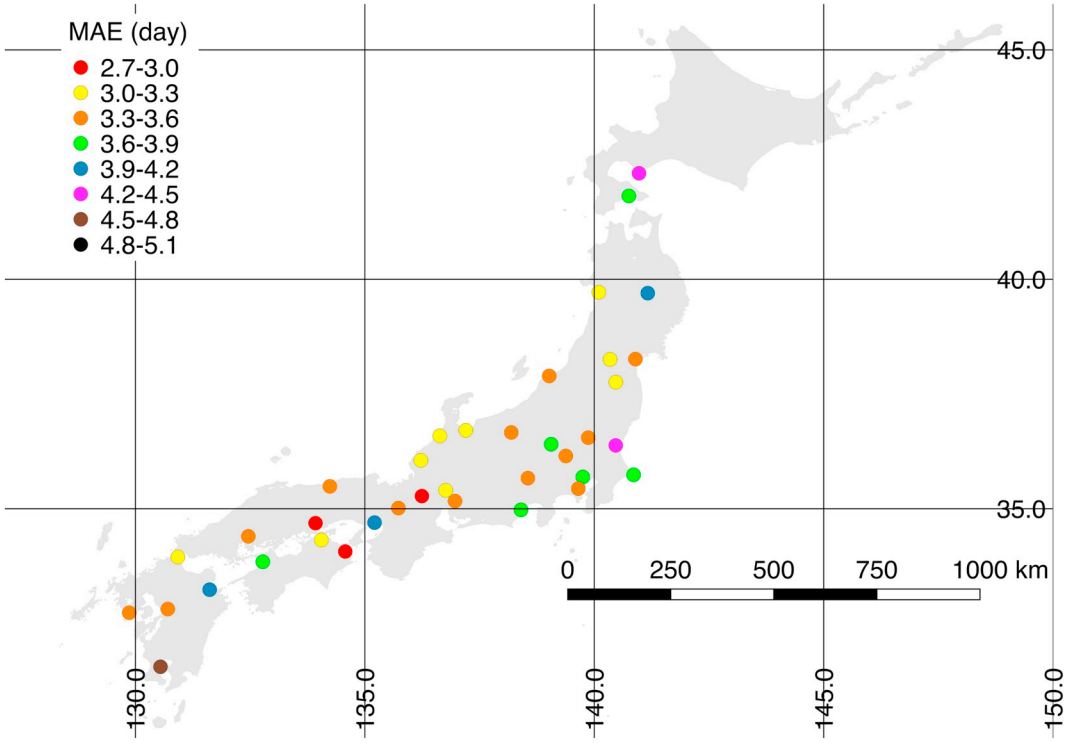

Fig. 4. (*continued*)

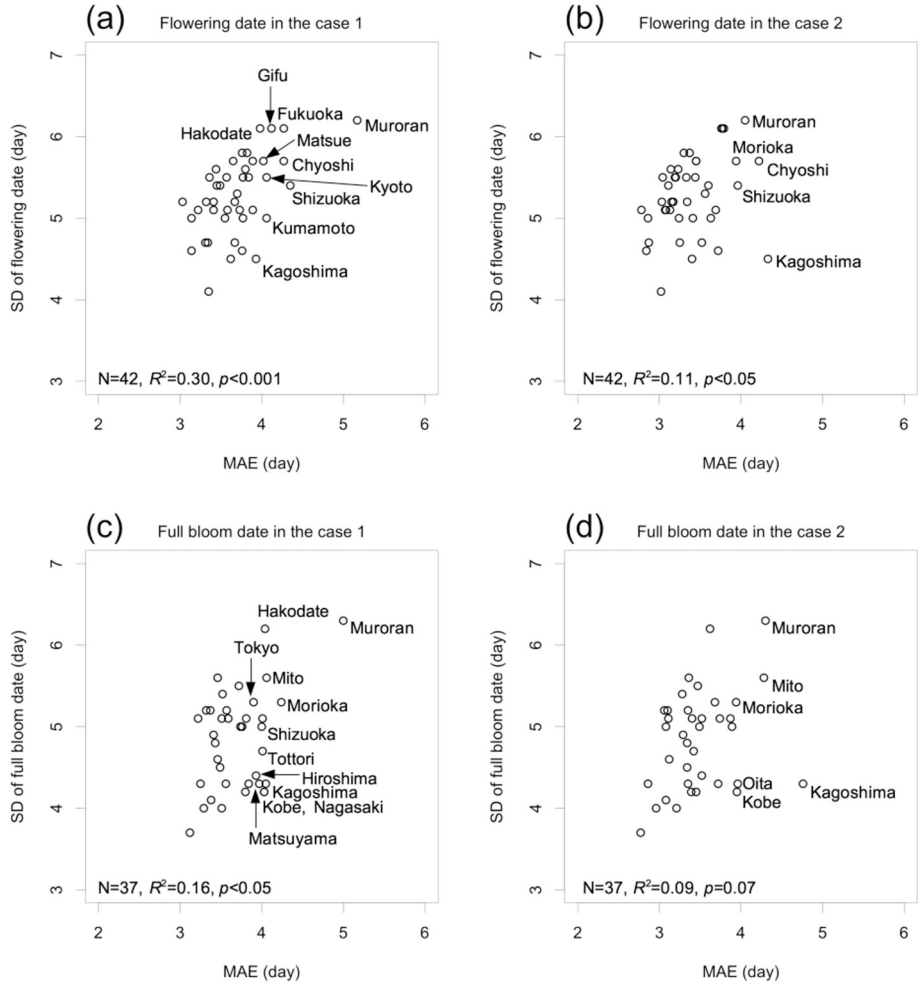

Fig. 5. Relationship between MAEs between observed and predicted flowering and full bloom dates in Cases 1 and 2 of bidirectional SOM analysis, and (a, c) standard deviations (SD) of observed flowering and (b, d) full bloom dates. We showed the cities whose MAEs between observed and predicted flowering and full bloom dates were ≥ 3.9.

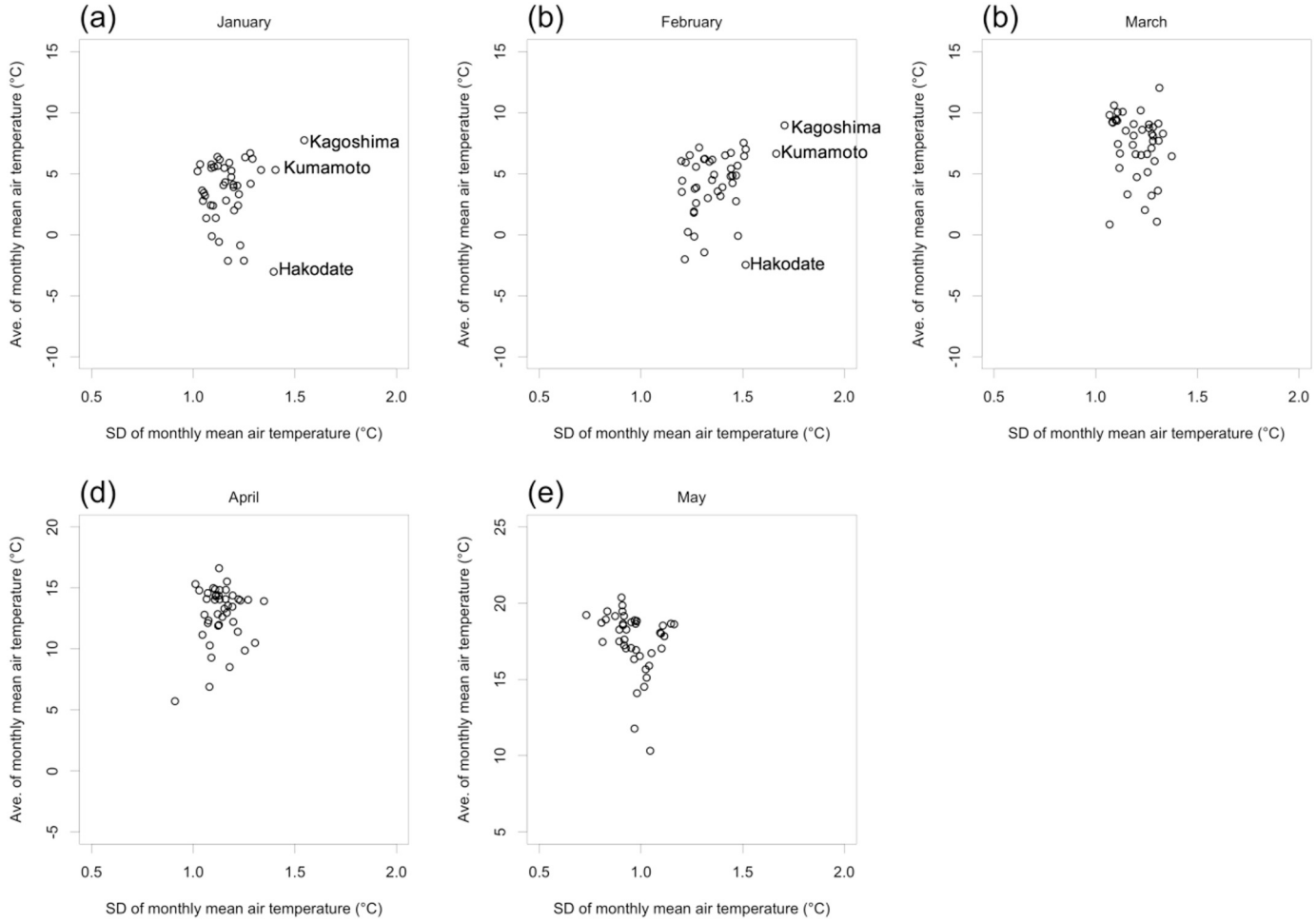

Fig. 6. Relationship between averages and standard deviations (SD) of monthly mean air temperature from 1953 to 2018 (a: Jan, b: Feb., c: Mar., d: Apr., e: May). We used the monthly mean air temperature data observed at 42 stations of the JMA's AMeDAS (JMA, 2019c).

Acknowledgements

This study was conducted with funding from a Joint Usage/ Research Grant from the River Basin Research Center (2018-F-002), Gifu University in Japan. We thank the editor and anonymous reviewer for their kind and constructive comments.

References

Aono, Y., Moriya, C., 2003. A generalized model to estimate flowering for cherry tree (*Prunus yedoensis*) considering both processes of endodormancy completion and development. J. Agric. Meteorol. 59, 165–177 (in Japanese with English summary).

Asakura, T., Sugiura, H., Sakamoto, D., Sugiura, T., Gemma, H., 2010. A universal model for predicting the full bloom date of Japanese flowering cherry. J. Agric. Meteorol. 66 (4), 269–277 (in Japanese with English summary).

Badeck, F.-W., Bondeau, A., Böttcher, K., Doktor, D., Lucht, W., Schaber, J., Sitch, S., 2004. Responses of spring phenology to climate change. New Phytol. 162, 295–309.

Basler, D., 2016. Evaluating phenological models for the prediction of leaf-out dates in six temperate tree species across Central Europe. Agric. For. Meteorol. 217, 10–21.

Campoy, J.A., Darbyshire, R., Dirlewanger, E., Quero-García, J., Wenden, B., 2018. Yield potential definition of the chilling accumulation reveals likely underestimation of the risk of climate change on winter chill accumulation. Int. J. Biometeorol. https://doi.org/10.1007/s00484-018-1649-5.

Cesaraccio, C., Spano, D., Snyder, R.L., Duce, P., 2004. Chilling and forcing model to predict bud-burst of crop and forest species. Agric. For. Meteorol. 126, 1–13.

Chuine, I., Bonhomme, M., Legave, J.-M., García de Cortázar-Atauri, I., Charrier, G., Lacointe, A., Améglio, T., 2016. Can phenological models predict tree phenology accurately in the future? The unrevealed hurdle of endodormancy break. Glob. Chang. Biol. 22, 3444–3460.

Chung, U., Mack, L., Yun, J.I., Kim, S.-H., 2011. Predicting the timing of cherry blossoms in Washington, DC and mid-Atlantic states in response to climate change. PLoS One 6 (11), e27439. https://doi.org/10.1371/journal.pone.0027439.

Donnelly, A., Yu, R., 2017. The rise of phenology with climate change: an evaluation of IJB publications. Int. J. Biometeorol. 61, 29–50.

Fu, Y.H., Campioli, M., Deckmyn, G., Janssens, I.A., 2012. The impact of winter and spring temperatures on temperate tree budburst dates: results from an experimental climate manipulation. PLoS One 7 (10), e47324. https://doi.org/10.1371/journal.pone.0047324.

Fujisawa, M., Kobayashi, K., 2010. Apple (*Malus pumila var. domestica*) phenology is advancing due to rising air temperature in northern Japan. Glob. Chang. Biol. 16, 2651–2660.

Gao, F., Wang, Y., Hu, X., 2019. Evaluation of the suitability of Landsat, MERIS, and MODIS for identifying T spatial distribution patterns of total suspended matter from a self-organizing map (SOM) perspective. Catena 172, 699–710.

Harrington, C., Gould, P.J., 2015. Tradeoffs between chilling and forcing in satisfying dormancy requirements for Pacific northwest tree species. Front. Plant Sci. 6 (120). https://doi.org/10.3389/fpls.2015.00120.

Hudson, I.L., Keatley, M.R., Lee, S.Y., 2011. Using self-Organising maps (SOMs) to assess synchronies: an application to historical eucalypt flowering records. Int. J. Biometeorol. 55, 879–904.

Inoue, T., Nagai, S., 2015. Influence of temperature change on plant tourism in Japan: a case study of the flowering of *Lycoris radiata* (red spider lily). Jpn. J. Biometeorol. 52 (4), 175–184.

Japan Meteorological Agency (JMA), 2019a. Biometeorological information (in Japanese). Available online. http://www.data.jma.go.jp/sakura/data/index.html (accessed 24 Sept. 2019).

Japan Meteorological Agency (JMA), 2019b. Blooming and full blooming dates in cherry trees (in Japanese). Available online. http://www.data.jma.go.jp/sakura/data/sakura2012.pdf (accessed 24 Sept. 2019).

Japan Meteorological Agency (JMA), 2019c. Observed meteorological data by the Automated Meteorological Data Acquisition System (AMeDAS). Available online. https://www.data.jma.go.jp/gmd/risk/obsdl/index.php (accessed 24 Sept. 2019).

Jeong, J.-H., Ho, C.-H., Linderholm, H.W., Jeong, S.-J., Chen, D., Choi, Y.-S., 2011. Impact of urban warming on earlier spring flowering in Korea. Int. J. Climatol. 31, 1488–1497.

Kai, K., Kainuma, M., Murakoshi, N., Omasa, K., 1993. Potential effects on the phenological observation of plants by global warming in Japan. J. Agric. Meteorol. 48 (5), 771–774.

Kim, J.-H., Kim, S.-O., Kim, D.-J., Moon, K.H., Yun, J.I., 2015. Using daily temperature to

predict phenology trends in spring flowers. Asia-Pac. J. Atmos. Sci. 51 (2), 167–172.
Kohonen, T., 1982. Self-organized formation of topologically correct feature maps. Biol. Cybern. 43, 59–69.
Kohonen, T., 1990. The self-organizing map. Proc. IEEE 78 (9), 1464–1480.
Körner, C., Basler, D., 2010. Phenology under global warming. Science 327, 1461. https://doi.org/10.1126/science.1186473.
Kudo, G., 2014. Vulnerability of phenological synchrony between plants and pollinators in an alpine ecosystem. Ecol. Res. 29, 571–581.
Linderholm, H.W., 2006. Growing season changes in the last century. Agric. For. Meteorol. 137, 1–14.
Luedeling, E., Kunz, A., Blanke, M.M., 2013. Identification of chilling and heat requirements of cherry trees—a statistical approach. Int. J. Biometeorol. 57, 679–689.
Maruoka, T., Itoh, H., 2009. Impact of global warming on flowering of cherry trees (*Prunus yedoensis*) in Japan. J. Agric. Meteorol. 65 (3), 283–296 (in Japanese with English summary).
Menzel, A., Sparks, T.H., Estrella, N., et al., 2006. European phenological response to climate change matches the warming pattern. Glob. Chang. Biol. 12 (10), 1969–1976.
Miller-Rushing, A.J., Katsuki, T., Primack, R.B., Ishii, Y., Lee, S.D., Higuchi, H., 2007. Impact of global warming on a group of related species and their hybrids: cherry tree (Rosaceae) flowering at Mt. Takao, Japan. Am. J. Bot. 94, 1470–1478.
Peñuelas, J., Rutishauser, T., Filell, I., 2009. Phenology feedbacks on climate change. Science 324, 887–888.
Pérez-Hoyos, A., Martínez, B., García-Haro, F.J., Moreno, A., Gilabert, M.A., 2014. Identification of ecosystem functional types from coarse resolution imagery using a self-organizing map approach: a case study for Spain. Remote Sens. 6, 11391–11419. https://doi.org/10.3390/rs61111391.
R Project for Statistical Computing, 2019. https://www.r-project.org (accessed 24 Sept. 2019).
Richardson, A.D., Keenan, T.F., Migliavacca, M., Ryu, Y., Sonnentag, O., Toomey, M., 2013. Climate change, phenology, and phenological control of vegetation feedbacks to the climate system. Agric. For. Meteorol. 169, 156–173.
Sakurai, R., Jacobson, S.K., Kobori, H., Primack, R., Oka, K., Komatsu, N., Machida, R., 2011. Culture and climate change: Japanese cherry blossom festivals and stakeholders' knowledge and attitudes about global climate change. Biol. Conserv. 144, 654–658.
Sparks, T.H., 2014. Local-scale adaptation to climate change: the village flower festival. Climate Change 60, 87–89.
Templ, B., Koch, E., Bolmgren, K., et al., 2018. Pan European Phenological database (PEP725): a single point of access for European data. Int. J. Biometeorol. 62, 1109–1113.
Wang, H., Ge, Q., Dai, J., Tao, Z., 2015a. Geographical pattern in first bloom variability and its relation to temperature sensitivity in the USA and China. Int. J. Biometeorol. 59 (8), 961–969.
Wang, H., Ge, Q., Rutishauser, T., Dai, Y., Dai, J., 2015b. Parameterization of temperature sensitivity of spring phenology and its application in explaining diverse phenological responses to temperature change. Sci. Rep. 5, 8833. https://doi.org/10.1038/srep08833.
Wang, L., Ning, Z., Wang, H., Ge, Q., 2017. Impact of climate variability on flowering phenology and its implications for the schedule of blossom festivals. Sustainability 9, 1127. https://doi.org/10.3390/su9071127.
Wenden, B., Campoy, J.A., Lecourt, J., et al., 2016. Data descriptor: A collection of European sweet cherry phenology data for assessing climate change. Sci. Data 3, 160108. https://doi.org/10.1038/sdata.2016.108.